

## Wind-induced vibration characteristics and parametric analysis of large hyperbolic cooling towers with different feature sizes

Shitang Ke<sup>\*1,2</sup>, Yaojun Ge<sup>2a</sup>, Lin Zhao<sup>2b</sup> and Yukio Tamura<sup>3c</sup>

<sup>1</sup>Department of Civil Engineering, Nanjing University of Aeronautics and Astronautics, 29 Yudao Road, Nanjing 210016, China

<sup>2</sup>State Key Laboratory for Disaster Reduction in Civil Engineering, Tongji University, 1239 Siping Road, Shanghai 200092, China

<sup>3</sup>Center of Wind Engineering Research, Tokyo Polytechnic University, 1583 Iiyama, Atsugi, Kanagawa 243-0297, Japan

(Received July 6, 2014, Revised November 29, 2014, Accepted December 16, 2014)

**Abstract.** For a systematic study on wind-induced vibration characteristics of large hyperbolic cooling towers with different feature sizes, the pressure measurement tests are finished on the rigid body models of three representative cooling towers with the height of 155 m, 177 m and 215 m respectively. Combining the refined frequency-domain algorithm of wind-induced responses, the wind-induced average response, resonant response, background response, coupling response and wind vibration coefficients of large cooling towers with different feature sizes are obtained. Based on the calculating results, the parametric analysis on wind-induced vibration of cooling towers is carried out, e.g. the feature sizes, damping ratio and the interference effect of surrounding buildings. The discussion shows that the increase of feature sizes makes wind-induced average response and fluctuating response larger correspondingly, and the proportion of resonant response also gradually increased, but it has little effect on the wind vibration coefficient. The increase of damping ratio makes resonant response and the wind vibration coefficient decreases obviously, which brings about no effect on average response and background response. The interference effect of surrounding buildings makes the fluctuating response and wind vibration coefficient increased significantly, furthermore, the increase ranges of resonant response is greater than background response.

**Keywords:** large hyperbolic cooling towers; wind tunnel test; wind-induced vibration characteristics; wind vibration coefficient; parametric analysis

### 1. Introduction

Along with the adjustment of national energy industry, increasing generating set, and the rapid development of nuclear power construction, the super large hyperbolic cooling tower, whose

---

\*Corresponding author, Associate Professor, E-mail: keshitang@163.com

<sup>a</sup>Professor, E-mail: tgwang@nuaa.edu.cn

<sup>b</sup>Professor, E-mail: yaojunge@tongji.edu.cn

<sup>c</sup>Professor, E-mail: yukio@arch.t-kougei.ac.jp

height breaks the world record of 200 m, has been put on construction schedule. To achieve leapfrog development of large cooling towers, the wind-induced vibration safety issues of that structure is the bottleneck problem to be solved. Once the large cooling tower, one of the important structures as a nuclear power and thermal power plants, is destructive, the influence of destruction is very large and the consequence is unimaginable (Harte and Wittek 2009). So further study on the wind-induced vibration responses characteristics of large cooling towers and vibration mechanism are of great significance.

Since three of the eight cooling towers with the height of 115 m at British bridge power plant collapsed in 1965, the research on the wind resistance of cooling towers was carried out throughout the world, but the wind-resistant research of cooling towers began in 1983 in China. Mainly involved in the wind-resistant researches are as follows: the surface distribution characteristics of wind loads on the cooling towers (Niemann and Kopper 1998, Sun and Gu 1992), interference effect of cooling towers group and surrounding buildings (Orlando 2001, Bartoli *et al.* 1997), random wind-induced responses of the cooling towers (Busch *et al.* 2002, Li and Cao 2013), the equivalent static wind loads (Zhang *et al.* 2014, Ramakrishnan 2012), wind-induced stability of cooling towers (Goodarzi 2010, Noh *et al.* 2003, Zahlten and Borri 1998). These research results provided good guidance to the wind-resistant design for large cooling towers at the same time. However, those research results couldn't solve the wind-resistance design problem of under construction or planned cooling towers with the height excess of the 200 m world record. Wind vibration mechanism of this kind of super large cooling tower is needed to be more deeply studied.

In fact, Wind vibration responses of the cooling towers depend on the structure dynamic characteristics and the external load excitation, such as the change of structural feature sizes and damping ratio affecting the size of average response, resonance response and background response or that affecting the wind vibration coefficient and distribution characteristics. When the interference of surrounding buildings is taken into account, the resonant effect of the cooling tower is increasingly prominent, and the action mechanism of wind vibration will also be more complicated. At home and abroad, structural wind-resistant studies of large cooling towers less involve the wind-induced vibration mechanism. In view of this, three large hyperbolic cooling towers with different feature sizes are taken as examples, wind tunnel tests of the rigid model for pressure measurement are respectively carried out to obtain the surface fluctuating wind pressure distributions. Based on the refined method of the dynamic response of the wind-induced vibration for the large hyperbolic cooling tower, namely, consistent coupling method, the parametric analysis of feature sizes, damping ratio and the interference factors under the action of the strong wind are discussed. Ultimately, the wind-induced vibration mechanism of large hyperbolic cooling towers with different feature sizes is revealed, and some beneficial conclusions are obtained for wind-resistant design of large hyperbolic cooling towers.

## 2. The refined calculation method of wind-induced responses

Existing studies (Zahlten and Borri 1998, Zhao and Ge 2010) have shown that wind-induced vibration of large cooling towers has three characteristics, such as multiple load form, multiple modal participation and multiple coupling effects. The traditional complete quadratic combination (CQC) method can't accurately analyze the wind-induced mechanism of structures, and three components method (LRC+IWL) with the background and resonant separately to solve ignores the

cross terms between the background and the resonance. Therefore, the consistent coupled method (CCM), fully considering the background, resonant responses and the cross term between the background and the resonance responses, was put forward. The CCM method could solve vibration responses and equivalent static wind load, which has successfully applied on the wind-induced vibration analysis of many super large cooling towers in the domestic and foreign. The main derivation and validation process of CCM method are given below:

### 2.1 Refined expressions of total coupled method

The dynamic response of a cooling tower to turbulent wind excitation can be expressed in terms of the matrix equations

$$M\ddot{y} + C\dot{y} + Ky = Tp(t) \tag{1}$$

where  $p$  means external stochastic wind load vector;  $M$ ,  $C$ ,  $K$  means Mass, damping and stiffness matrix, respectively;  $T$  means Force indicating matrix that is used to match the dimension number of nodes number and external load vector.

Using the modal coordinates, the dynamic displacement can be represented as

$$y(t) = \Phi q(t) = \sum_{i=1}^n \phi_i q_i(t) = \sum_{i=1}^m \phi_i q_i(t) + \sum_{i=m+1}^n \phi_i q_i(t) = y_d + y_s \tag{2}$$

where  $y_d$  = the response considering the background and resonant contribution of former  $m$  modes,  $y_s$  = the response only considering quasi-static contribution of remaining modes,  $q$  = generalized displacement vector, and  $\Phi$  = Matrix of modes of vibration.

The static response is  $K^{-1}P(t)$  under the wind loads vector  $P(t)$ , unfolded as

$$K^{-1}p(t) = \sum_{i=1}^n F_i p(t) = \sum_{i=1}^m F_i p(t) + \sum_{i=m+1}^n F_i p(t) \tag{3}$$

where  $F_i$  = flexibility matrix of the  $i_{th}$  mode, given by

$$F_i = \frac{\phi_i \phi_i^T}{\phi_i^T K \phi_i} \tag{4}$$

$y_s$  is expressed by

$$y_s = \sum_{i=m+1}^n F_i p(t) = K^{-1}p(t) - \sum_{i=1}^m F_i p(t) \tag{5}$$

Combine Eq. (2) and Eq. (5),  $y(t)$  is expressed as

$$\begin{aligned} y(t) &= y_d + y_s = \sum_{i=1}^m \phi_i q_i(t) + K^{-1}p(t) - \sum_{i=1}^m F_i p(t) \\ &= \sum_{i=1}^m (\phi_i q_i(t) - F_i p(t)) + K^{-1}p(t) \end{aligned} \tag{6}$$

Accordingly, the background and resonant responses are given by

$$y(t)_b = K^{-1}p(t) \tag{7}$$

$$y(t)_r = \sum_{i=1}^m (\phi_i q_i(t) - F_i p(t)) \tag{8}$$

And  $\sigma_r$ = root-mean-square (RMS) value of  $y(t)$ , is expressed by

$$\sigma_t = \sqrt{\sigma_r^2 + \sigma_b^2 + 2\rho_{r,b}\sigma_r\sigma_b} = \sqrt{\sigma_r^2 + \sigma_b^2 + \sigma_c^2} \tag{9}$$

where  $\sigma_b, \sigma_r, \sigma_c$ = response component vector of background, resonant and coupled term, respectively, and  $\rho_{r,b}$ = correlation coefficient between background and resonant component, is given by

$$\rho_{r,b} = \frac{\sigma_{r,b}^2}{\sigma_r\sigma_b} = \frac{\int \sum_{j=1}^n \sum_{k=1}^n \phi_{j,i} \phi_{k,i} S_{q_{b,j}, q_{r,k}}(\omega) d\omega}{\text{sqrt}(\int \sum_{j=1}^n \sum_{k=1}^n \phi_{j,i} \phi_{k,i} S_{q_{r,j}, q_{r,k}}(\omega) d\omega) \int \sum_{j=1}^n \sum_{k=1}^n \phi_{j,i} \phi_{k,i} S_{q_{b,j}, q_{b,k}}(\omega) d\omega)} \tag{10}$$

It can be found in Eq. (9) that fluctuating wind-induced responses should include background, resonant and coupled component between the former two terms. However, the tri-component method based on SRSS combination cannot consider the coupled component, which is acceptable for the small value of  $\rho_{r,b}$ , but widely different for some throng coupled structures (Ke *et al.* 2012). Due to the complex calculation process of Eq. (10), the approach of solving coupled component based on covariance matrix of coupled restoring force in this paper is presented.

### 2.2 Covariance matrix of resonant (background, coupled and generalized) Elastic restoring force

The generalized displacement response of the  $i_{th}$  mode only containing resonant component from (8) is given by

$$q_{r,i}(t) = q_i(t) - \frac{\phi_i^T p(t)}{\phi_i^T K \phi_i} = q_i(t) - \frac{F_i(t)}{K_i} \tag{11}$$

Accordingly, the cross-power spectrum of generalized resonant displacement between the  $i_{th}$  mode and the  $j_{th}$  mode is expressed as

$$\begin{aligned} S_{q_{r,i}, q_{r,j}}(\omega) &= \int_{-\infty}^{\infty} R_{q_{r,i}, q_{r,j}}(\tau) e^{-i2\pi\omega\tau} d\tau = \int_{-\infty}^{\infty} E[q_{r,i}(t), q_{r,j}(t+\tau)] e^{-i2\pi\omega\tau} d\tau \\ &= \int_{-\infty}^{\infty} E[(\int_{-\infty}^{\infty} h_i(u) F_i(t-u) du - \frac{F_i(t)}{K_i})(\int_{-\infty}^{\infty} h_j(v) F_j(t+\tau-v) dv - \frac{F_j(t+\tau)}{K_j})] e^{-i2\pi\omega\tau} d\tau \tag{12} \\ &= (H_i^*(\omega) - \frac{1}{K_i})(H_j(\omega) - \frac{1}{K_j}) S_{F_i, F_j}(\omega) = H_{r,i}^*(\omega) H_{r,j}(\omega) S_{F_i, F_j}(\omega) \end{aligned}$$

where  $H_{r,i} = H_i(\omega) - 1/K_i$ , is the resonant transfer function of the  $i_{th}$  mode.  $K_i$ = stiffness matrix of the  $i_{th}$  mode, which can be expressed as

$$K_i = \frac{\phi_i^T K \phi_i}{\phi_i \phi_i^T} \tag{13}$$

The covariance of generalized resonant response is given by

$$C_{qq,r} = \int_{-\infty}^{\infty} H_r^* S_{FF} H_r d\omega = \int_{-\infty}^{\infty} H_r^* \Phi^T T D S_{AA} D^T T^T \Phi H_r d\omega \quad (14)$$

where  $\mathbf{A}$ ,  $\mathbf{D}$ = time coordinate vector and proper modes matrix with POD method (Holmes 2002),  $S_{AA}$  is the matrix of the cross power spectra for time coordinate vectors  $\mathbf{A}$ . Because the dimension number of  $\mathbf{p}(t)$  is very large, so the POD method is used to reduce the dimension number of  $\mathbf{p}(t)$  and save computing time.

And accordingly, the resonant elastic restoring force vector can be represented as

$$P_{eqq,r} = Ky(t)_r = K\Phi q(t)_r = M\Phi\Lambda q(t)_r \quad (15)$$

The cross-covariance matrix  $C_{pp,r}$  of  $P_{eqq,r}$  is expressed as

$$\begin{aligned} C_{pp,r} &= \overline{P_{eqq,r} P_{eqq,r}} = M\Phi\Lambda \overline{q(t)_r q(t)_r} \Lambda^T \Phi^T M^T \\ &= M\Phi\Lambda C_{qq,r} \Lambda^T \Phi^T M^T \end{aligned} \quad (16)$$

It can be easily seen from Eq. (14) and Eq. (15) that the accuracy of  $P_{eqq,r}$  is determined by the number of calculating mode and dynamic characteristic of structure, and  $C_{pp,t}$ = the covariance matrix of total fluctuating elastic restoring force, can be obtained with Eq. (16) as long as resonant transfer function  $H_r$  is replaced by generalized transfer function  $\mathbf{H}$ . In this paper, in order to calculate coupled component, the covariance matrix of coupled elastic restoring force  $C_{pp,c}$  is defined, which is given by

$$C_{pp,c} = C_{pp,t} - (C_{pp,b} + C_{pp,r}) \quad (17)$$

### 2.3 Wind-induced response of resonant, background and cross term

It is clear that the resonant and coupled response can be regarded as the quasi-static response under the inertial load excitation. Thus, the resonant and coupled response can be obtained using LRC method (Kasperski and Niemann 1992), take the resonant component as the example, an arbitrary dynamic response of interest  $r(t)$  is given by

$$r(t)_r = IP_{eqq,r} \quad (18)$$

And the covariance matrix of resonant response  $r(t)$  is expressed as

$$C_{rr,r} = \overline{r(t)_r r(t)_r} = IC_{pp,r} I^T = IM\Phi\Lambda C_{qq,r} \Lambda^T \Phi^T M^T I^T \quad (19)$$

where  $\Lambda = \text{diag}(\omega_1^2, \dots, \omega_m^2)$ . The RMS value vector of resonant response is given by

$$\sigma_{R,r} = \sqrt{\text{diag}(C_{rr,r})} \quad (20)$$

where  $\text{diag}(\cdot)$ = the column vector of diagonal elements of  $C_{rr,r}$ .

Accordingly, if the  $C_{rr,r}$  is replaced with  $C_{rr,b}$ ,  $C_{rr,c}$ ,  $C_{rr,t}$ , we can obtain background, coupled and total fluctuating wind-induced response using the same thought. It is worth noting that the value of covariance matrix of coupled component using Eq. (19) might be minus, which indicates that calculation with tri-component method will overrate the value of response. However, absolute

value of these elements of  $C_{rr,c}$  should be adopted in Eq. (20), but in combination of total response of the influence of minus must be considered.

#### 2.4 Combination of consistent coupled method

The total fluctuating response can be given by

$$\sigma_t = \sqrt{\sigma_r^2 + \sigma_b^2 + \text{sign}(\text{diag}(C_{rr,c}))\sigma_c^2} \quad (21)$$

Accordingly, the totally response of the tower is then given by

$$R_a = \bar{R} + g \times \sqrt{\sigma_r^2 + \sigma_b^2 + \text{sign}(\text{diag}(C_{rr,c}))\sigma_c^2} \quad (22)$$

where  $R_a$  is the total wind induced response which contains the mean term, background term, resonant term and cross term.  $g$  is the peak factor, and is expressed by

$$g = \sqrt{2 \ln vT} + \frac{\gamma}{\sqrt{2 \ln vT}} \quad (23)$$

where  $T=600$  s,  $\gamma$  is Euler's constant, and is 0.5772. The research demonstrates that the peak factor of large cooling towers is from 3.0 to 4.0 (Ke *et al.* 2013), so in the paper the whole peak factors are 3.5.

### 3. General situation of wind tunnel tests

#### 3.1 The introduction of project

Considering Chinese design specification for cooling towers applied to the maximum height 165 m (DL/T 5339-2006 2006), the British design standard for cooling towers “Code of practice for structural design and construction” applied to the maximum height 170 m, and Germany design specification for cooling towers VGB -R 610 Ue (VGB-Guideline 2005) giving no the applicable height scope, the Chinese nuclear power cooling towers to be built or under construction has gone far beyond the height. So it is necessary for the comparative study on the wind vibration response of the different characteristic size Cooling tower.

In general, the fundamental frequency is inversely proportional to the characteristic sizes of cooling towers. Therefore, three large hyperbolic cooling towers with different feature sizes from power plant actual engineering projects at home and abroad are analyzed, and the basic parameters of the cooling tower structure is as follows.

Example 1: 660 MW large cooling tower is in India TALWANDI power plant, the tower height is 155 m, the top diameter is 73 m, throat height is 119 m, the throat diameter is 68 m, the height of air inlet is 10.6 m, the diameter is 114 m, 46 cylinders of diameter of 1.1 m are used for herringbone column, and the structural fundamental frequency is 0.92 Hz.

Example 2: super large cooling tower of million kilowatts is in Chinese Zhejiang power plant, the tower height is 177 m, the top diameter is 86 m, throat height is 75 m, the throat diameter is 133 m, the height of air inlet is 16.5 m, a diameter is 122 m, 48 cylinders of diameter of 1.3 m are used for herringbone column, and the structural fundamental frequency is 0.82 Hz.

Example 3: super-large cooling tower is in Chinese Pengze nuclear power plant, the tower height is 215 m, throat height is 160 m, zero meters height is 170 m, the height of air inlet is 20.8 m, drench water area is 18300 m<sup>2</sup>, 48 cylinders of diameter of 1.8 are used for herringbone column, and the structural fundamental frequency is 0.68 Hz.

### 3.2 The wind tunnel tests

The fluctuating wind pressure acting on the shell surface was obtained from the wind tunnel tests. The tests were carried out in TJ-3 Boundary Layer Wind Tunnel in Tongji University. The geometry scale of the building models were 1:200, on which 12×36 measuring points were arranged. The pressure taps were connected with the measurement system through PVC tubing. To avoid the distortion of the dynamic pressure, the signals had been modified using the transfer function of the tubing systems. A DSM 3000 scan valve system was used to measure the wind pressures on the rigid model of the tower. The pressure signals were sampled at 312.5 Hz. Figs. 1 and 2 present the photograph of cooling towers in the wind tunnel test and measured points of outside wind pressures distribution.

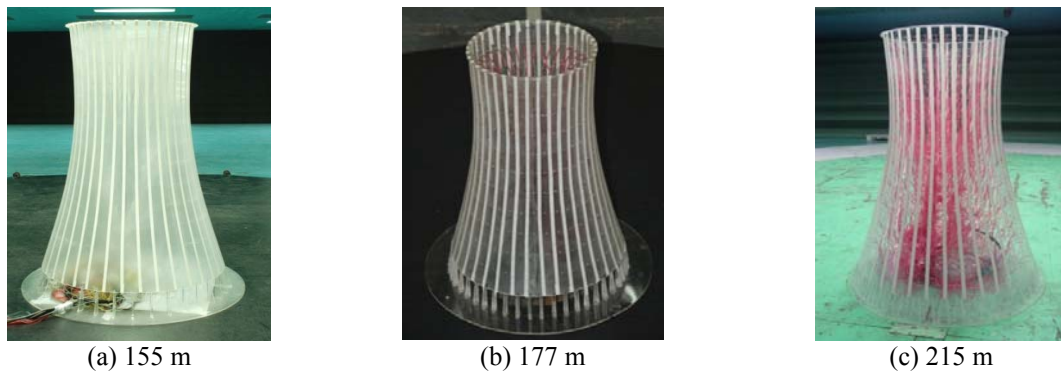


Fig. 1 The rigid models for measuring wind pressure of cooling towers with different heights

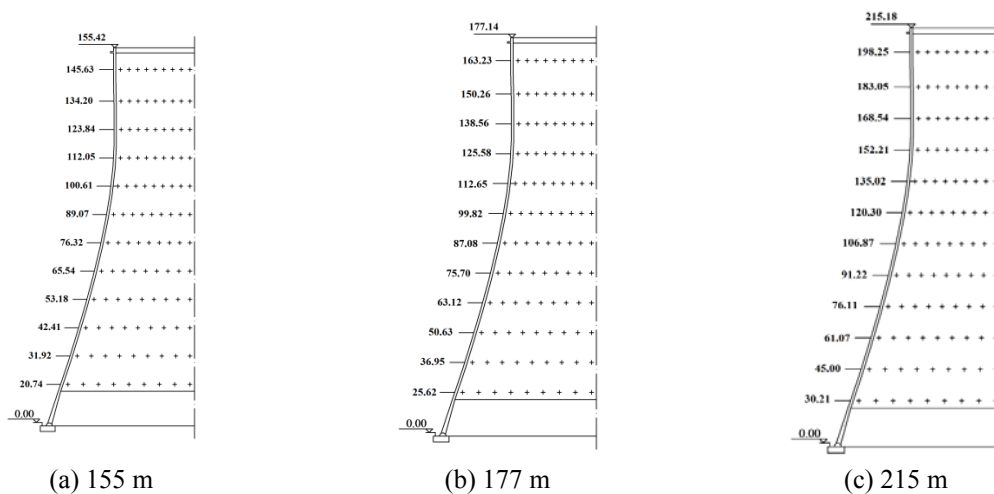


Fig. 2 The height and distribution of measured points for surface wind pressures

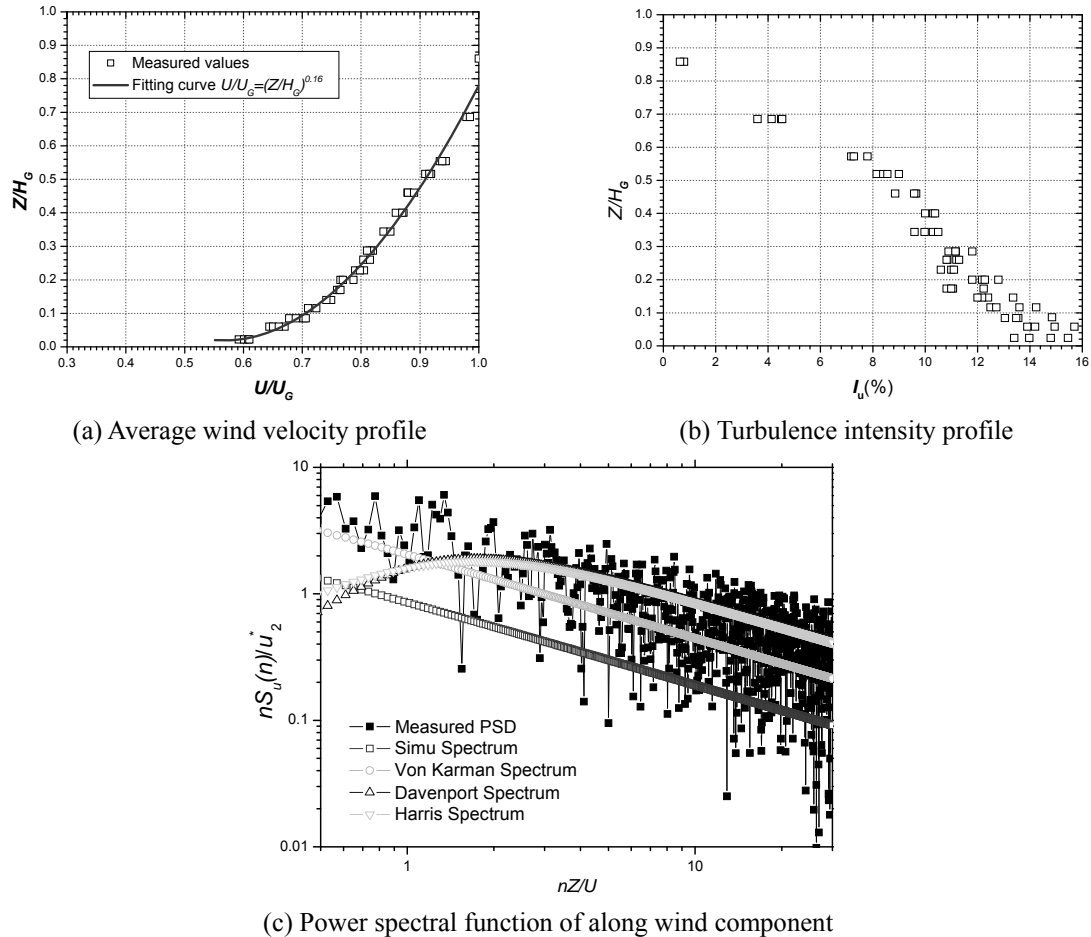


Fig. 3 Wind environment parameters of Type A terrain in TJ-3 wind tunnel

According to the surrounding building situation around tower, corresponding terrain category B defined in the Chinese code, was simulated in the wind tunnel with a scale ratio of 1:200 by a combination of turbulence generating spires and a barrier at the entrance of the wind tunnel, roughness elements along the wind tunnel floor upstream of the model. The exponent of the mean wind speed profile is 0.16, and the turbulent intensity is about 12% at the top of the tower. More information could be referred from Fig. 3.

Flow-induced forces on curved bodies, like cooling towers, depend strongly upon Reynolds number  $Re$  ( $Re=UD/\nu$ , where  $U$  is the mean velocity of the undisturbed flow,  $D$  is the tower diameter,  $\nu$  is the kinematic viscosity of air) and surface roughness.  $Re$  in the wind tunnel should be the same as in full-scale, however, adjusting velocity is impossible since the velocity in the tunnel should be 300 times the full-scale one according to the  $Re$  effect. Usually, the difference of the Reynolds number between wind tunnel and prototype can be overcome with modification of the model surface roughness (Goudarzi *et al.* 2008, Qiao *et al.* 2011), and the simulation targets about surface flow parameters, such as Maximum and Minimum pressure values and its angles, zero pressure angle, separation angle, Strouhal number, etc., can be referred to on-site

Table 1 Characteristics of surface average pressure distribution

Key parameters	values
Minimum pressure and its angles	$C_{P,max}=-1.627, \theta_{min}=\pm 70^\circ$
Maximum pressure and its angles	$C_{P,max}=1.0, \theta_{max}=0^\circ$
zero pressure angle	$\theta_{zero}=\pm 33^\circ$
separation angle	$\theta_{separation}=\pm 120^\circ$
Strouhal number	$S_t \geq 0.22$
Average pressure of wake flow	$C_{P,wake\ flow} \approx -0.4,$

measurement of full-scale cooling towers. In accordance with Chinese wind loading Codes, surface pressure distribution under post critical Reynolds condition is suggested as

$$\mu_p(\theta) = \sum_{k=0}^m a_k \cos k\theta \tag{11}$$

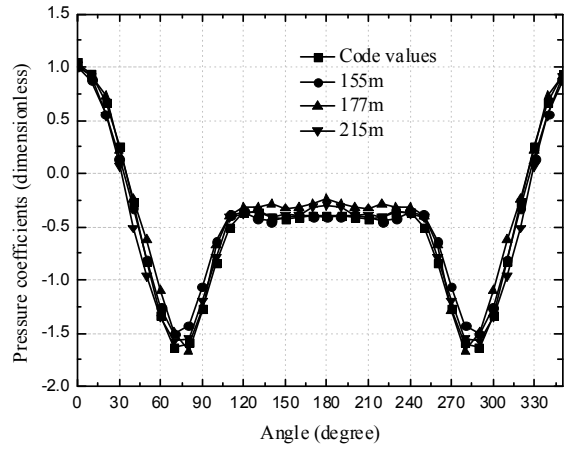
In which,  $\theta$  is the angle,  $m=7$ ,  $a_k$  is the fitting parameter ( $a_0=-0.4426, a_1=0.2451, a_2=0.6752, a_3=0.5356, a_4=0.0615, a_5=-0.1384, a_6=0.0014, a_7=0.0650$ ). The distribution curve was suggested by on-site measurement of two full-scale cooling towers with height of about 120 m in Guangdong Maoming in the 1980's, and some key parameters about average pressure function around cross section of cooling tower are listed in Table 1.

With the aid of sticking paper belts (10 mm width×0.1 mm depth, see Fig. 1) along vertical direction and adjusting incoming wind velocity, the actual aerodynamic characteristics of archetype cooling towers are successfully re-illustrated in the reduced-scale model with different models under lower Reynolds number, see Fig. 4. The average distribution and standard deviation of pressure coefficients were shown in Fig. 4(a) and 4(b) for three different models, the distribution showed well symmetry in absence of average distribution of pressure coefficients, but for the standard deviation of pressure coefficients, the distribution completely destroyed the symmetry, which is obviously different from the distribution characteristics of average value, and the values of standard deviation for 215 m model are higher than that of rigid model with 155 and 177 m models. We think that the non-symmetry and fluctuant characteristics of wind pressures could be obvious for cooling towers with larger feature sizes.

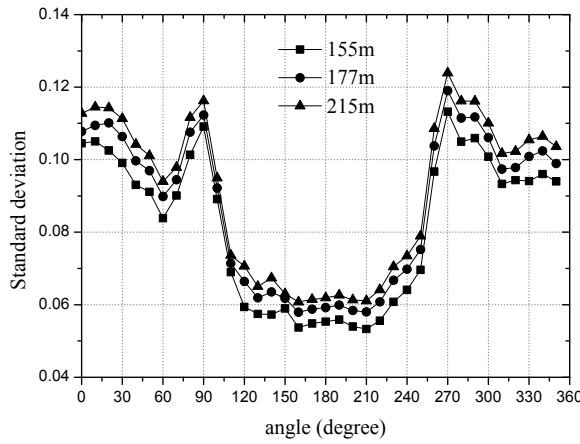
By measuring the tail flow velocity behind the cooling tower model with high-frequency anemometer, the main vortex shedding frequency through frequency-spectrum transformation of aerodynamic time history is obtained at 2.411 Hz. The Strouhal number based on the vortex shedding frequency of wake flow is 0.235, larger than 0.2, hence meeting the requirement of cooling tower reduced-scale models.

#### 4. The influence of feature sizes

Combining CCM method in this paper and wind tunnel results, the wind-induced dynamic responses are obtained. Fig. 5 shows the power spectrum curve of some typical nodes. It is noted that in number  $a-b$ ,  $a$ = the  $a$ th lay of the rigid body model of cooling tower and  $b$ = the  $b$ th node in the section  $a$  (see Fig. 2). It can be found from the figures that the resonant response component plays a comparatively important role in the total fluctuating response, and the contribution from

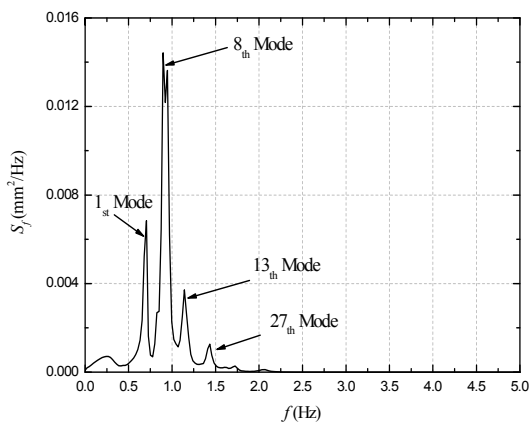


(a) Average pressure coefficients

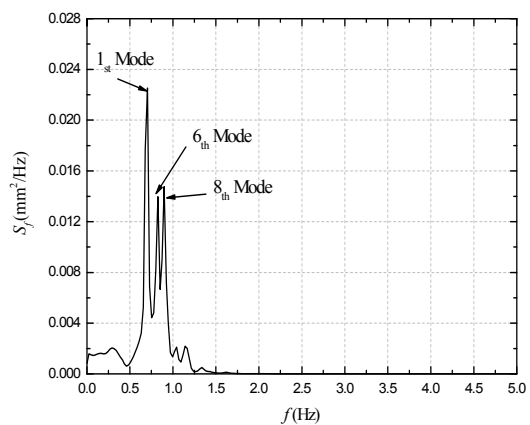


(b) Standard deviation of pressure coefficients

Fig. 4 Simulation of post critical Reynolds effect in three reduced-scale models



(a) node number 3-1



(b) node number 10-8

Fig. 5 Power spectrum of displacement at typical nodes on cooling tower

Table 2 The wind vibration response (mm) of typical nodes from different characteristic size cooling towers

node number		static response	fluctuating responses				peak factor	wind vibration coefficient
		average component	background component	resonant component	cross term	fluctuating component		
2-1 bottom	example 1	9.82	1.68	2.06	-0.97	2.47	3.63	1.91
	example 2	10.79	1.74	2.29	-1.10	2.66	3.88	1.96
	example 3	11.64	1.62	2.95	-1.30	3.10	3.82	2.02
6-4 middle	example 1	-12.48	1.76	2.58	-1.26	2.86	3.42	1.78
	example 2	-13.83	1.71	2.98	-1.48	3.10	3.58	1.80
	example 3	-15.08	1.87	3.23	-1.57	3.38	3.65	1.82
9-13 throat	example 1	0.89	1.04	2.35	0.69	2.66	3.64	11.88
	example 2	0.93	0.87	2.46	0.71	2.70	3.58	11.41
	example 3	1.04	0.60	2.84	0.75	3.00	3.57	11.26
12-27 top	example 1	4.52	1.76	3.28	0.26	3.73	3.64	4.00
	example 2	5.27	1.81	3.78	-0.82	4.11	3.83	3.99
	example 3	5.85	1.86	4.42	-0.76	4.73	3.75	4.03

background response induced by all modes should not be neglected, the contributions from the modes whose frequencies are higher than 2.5 Hz to the response are negligible.

From the analysis of wind-induced vibration of different cooling tower heights, it is clear that it is unreasonable to adopt a uniform wind vibration coefficient (see formula 12) for all sections of a structure to calculate wind-induced response as in current design codes. Table 2 gives the theoretical wind vibration coefficients computed by the peak responses, and then by comparison with the value of 1.9 fixed by the Chinese code, it can be seen that the dynamic wind-induced effects are more and more obvious with increment of height, and the wind vibration coefficient is mostly in the range from 1.4 to 3.0, which are the values fixed in codes. The value reached a maximum in the throat area. Thus, the author suggests that the wind vibration should be considered in a subsection.

$$\beta_{Li} = \frac{P_i}{P_{ei}} = 1 + \frac{gP_{fi}}{P_{ei}} \tag{12}$$

where  $P_i, P_{ei}, P_{fi}$  is total load, mean load and fluctuant load of node  $i$ ,  $g$  is the peak factor, which is expressed as

$$g = \bar{x}_e = \sqrt{2 \ln(vT)} + \frac{\gamma}{\sqrt{2 \ln(vT)}} \tag{13}$$

Many of the relationships above are quoted by the load specifications of Western countries, but the value method of the time  $T$  is slightly different, specifically  $T=3600s$  in the specifications of the United States and Canada, while AIJ1996 is 600s and  $T$  is defined as the observation time, so  $T$  shall be considered as the average time interval of the basic wind pressure, both the specification of China and the time interval of wind pressure of AIJ1996 are 10min, and therefore the  $T$  shall be 600s.  $v$  can approximately be the natural frequency of the first order, which is corresponding to the specification of China that when  $v= 0.0022Hz$ , the peak factor is reached to the minimum value of 1.52. When  $v$  is in the normal range of  $[0.1, 10]$ , the peak factor indicates a monotonically

increasing function related to  $\nu$ , and the value is mainly controlled in the range of [3.0, 4.5]. In the building structure load specification of China, the value of the peak factor is 2.2, which is significantly lower than the actual value, and the corresponding  $\nu$  is 0.01Hz at that, so that the value is obviously different to that of the actual structure.

In order to study the influence of the feature sizes of cooling towers on wind-induced responses, three examples are listed in Table 2. The table includes average wind-induced response, background response, resonant response, coupling term, total fluctuating response, peak factor and wind vibration coefficient of typical node. The node number is shown in Fig. 2, and  $a$ - $b$  means the measuring point  $b$  of the ring to rotate in counterclockwise direction at a cross section. Contrastive analysis can give the following conclusion:

(1) With the increase of feature sizes, the decrease of the structural fundamental frequency, the average response and the fluctuating response are gradually increased. The amplitude of the fluctuating response is greater than that of the average response at the nodes whose average response amplitude larger.

(2) From the fluctuating response in Table 2, for larger feature sizes and lower fundamental frequency of large cooling tower, the resonant response is obviously dominant, while the influence of the background response and cross terms is relatively weak. With the increase of the structural fundamental frequency, although resonant component is given priority to fluctuating response, the proportion of the background response is gradually increased. For the smaller feature size and low fundamental frequency of cooling tower structures, the quasi static contribution of wind load is more prominent, and the background response contribution of higher modes cannot be ignored.

(3) With the decrease of the fundamental frequency, the change range of the wind vibration coefficient of the four nodes listed in the table is not the same; but different from average or fluctuating response, the changing range of wind vibration coefficient of each node is relatively small. The reason is that the decrease of the structural fundamental frequency will increase the dynamic amplification effect of wind vibration response, making the increment of the fluctuating wind-induced response greater than that of average response. From another point of view, the fundamental frequency is decreased with the increase of the structure size in toroidal and meridian direction, leading to reduce the spatial correlation of fluctuating wind load on the surface, and making the wind vibration response relatively lower. The influence of these two factors on wind vibration response is just the opposite, which can lead that the change of the wind vibration coefficient of some nodes is small with the change of structural fundamental frequency.

## 5. The influence of damping ratio

Wind-induced response of large cooling tower structure is given priority to resonance component, and damping ratio, which has no effect on average response and background response, significantly influences the resonant components and cross terms between resonant response and background response. Thus the damping ratio will inevitably affect the total wind-induced response and wind vibration coefficient. In view of this, the wind-induced vibration of example 3 is analyzed with different damping ratio. Considering that the cooling tower is a typical reinforced concrete structure, the value range of the damping ratio for the structure is 0~5%. The parameters, 0.01, 0.02, 0.035 and 0.05, are respectively taken; and other calculation parameters are unchanged. Contour map of the resonance response and cross term of the shell structure is presented in Figs. 6 and 7 with different damping ratio.

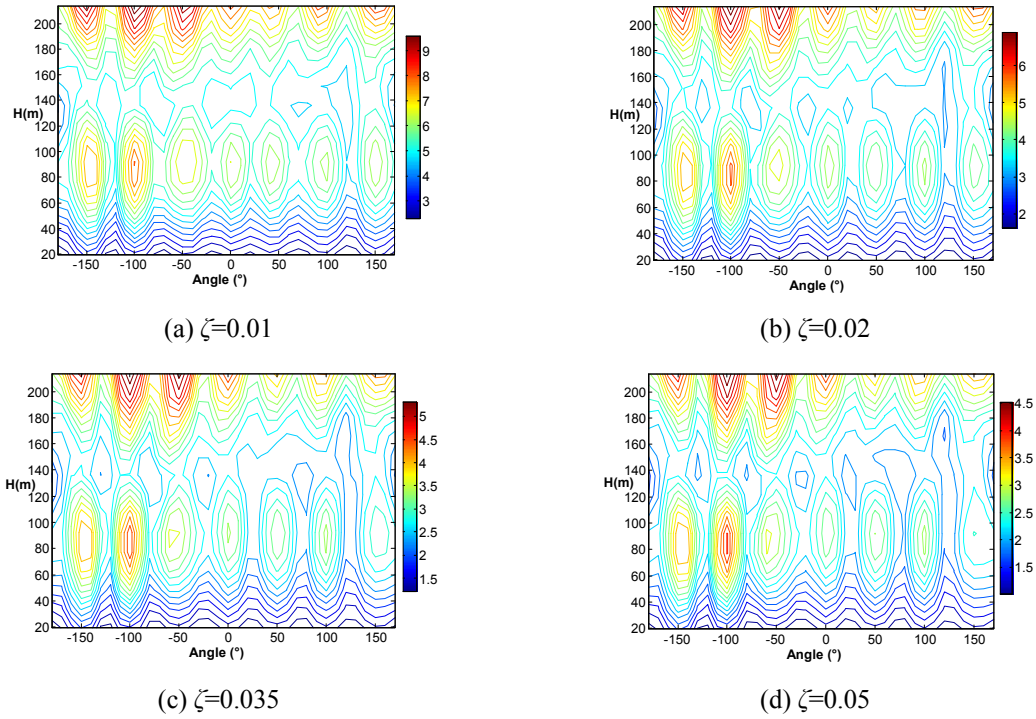


Fig. 6 The contour map of resonant response with different damping ratio

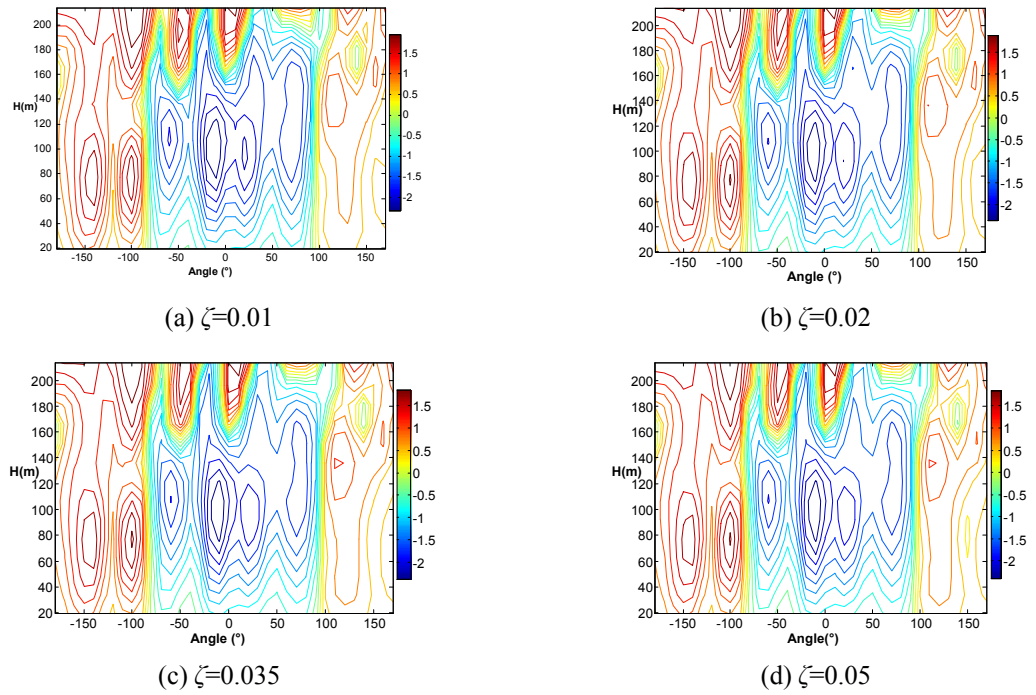


Fig. 7 The contour map of cross term with different damping ratio

Table 3 Comparison of components of wind-induced responses for typical nodes with different damping ratio

working condition of node		fluctuating response (mm)			wind vibration coefficient
node number	damping ratio	resonance component	cross terms	total pulse component	
3-1 tower bottom	0.01	2.92	0.46	4.25	2.01
	0.02	2.24	0.42	3.92	1.92
	0.035	1.68	0.39	3.42	1.83
	0.05	1.41	0.34	3.01	1.75
9-5 tower throat	0.01	5.17	-1.59	5.27	2.25
	0.02	3.61	-1.57	3.75	1.88
	0.035	2.73	-1.57	2.91	1.69
	0.05	2.29	-1.58	2.50	1.58
12-11 tower top	0.01	6.84	-0.60	7.06	5.23
	0.02	4.93	-0.72	5.22	4.15
	0.035	3.74	-0.79	4.10	3.51
	0.05	3.14	-0.84	3.55	3.14

It is noted that  $X$ -axis represents toroidal angle on the contour map in this paper;  $0^\circ$  is defined as the windward point, the clockwise rotation is defined as negative; counterclockwise rotation is positive;  $Y$ -axis means the height in meridian direction; and the change of color represents the numerical values of response component.

Through the comparison and analysis, the following conclusions are given.

(1) With the increase of damping ratio, the resonant response of the cooling tower significantly decreases, the peak of the resonant response reduces from 9.4 mm to 4.5 mm, the reason is that the resonant response is dominant in the wind vibration response of the large tower. However, the response distribution characteristics at the meridian height and the toroidal cross section is basic consistent, it is instructed that dominant mode stimulating the resonance response has not changed.

(2) The change for the distribution and value characteristics of the cross term response is not noticeable with the change of the damping ratio. That phenomenon shows that the relationship between the cross term response component of the structure and damping ratio is weak. The cross term response is more associated to fundamental frequency of the structure, vibration mode and load patterns.

The resonant response of the typical nodes, cross terms, total fluctuating response and wind vibration coefficient are showed in Table 3. It is found that total wind-induced fluctuating responses of the typical nodes are significantly reduced with the increase of damping ratio, and the average response of the structure remains the same, which will inevitably lead to reducing the wind vibration coefficient of the structure.

## 6. The influence of the surrounding interference

Considering the variability of cooling towers group combination and the complexity of surrounding buildings, the type of surrounding distracters cannot be specifically studied in this

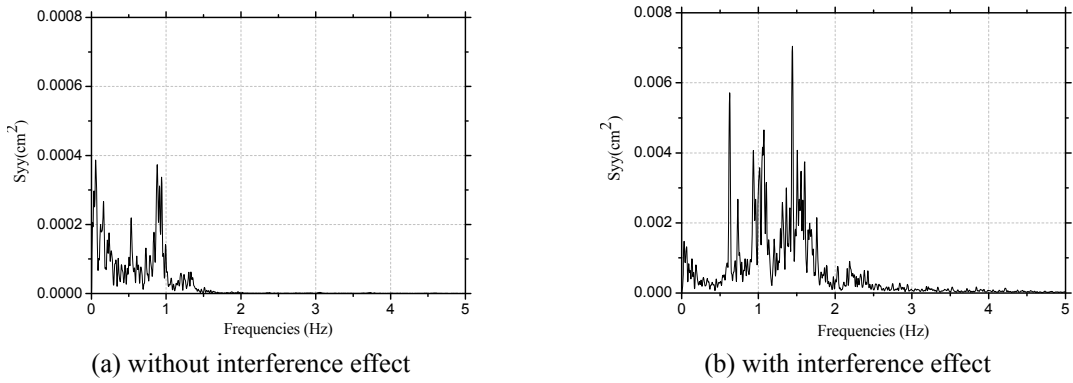


Fig. 8 Power spectrum density function of displacement on tower top with and without interference effect

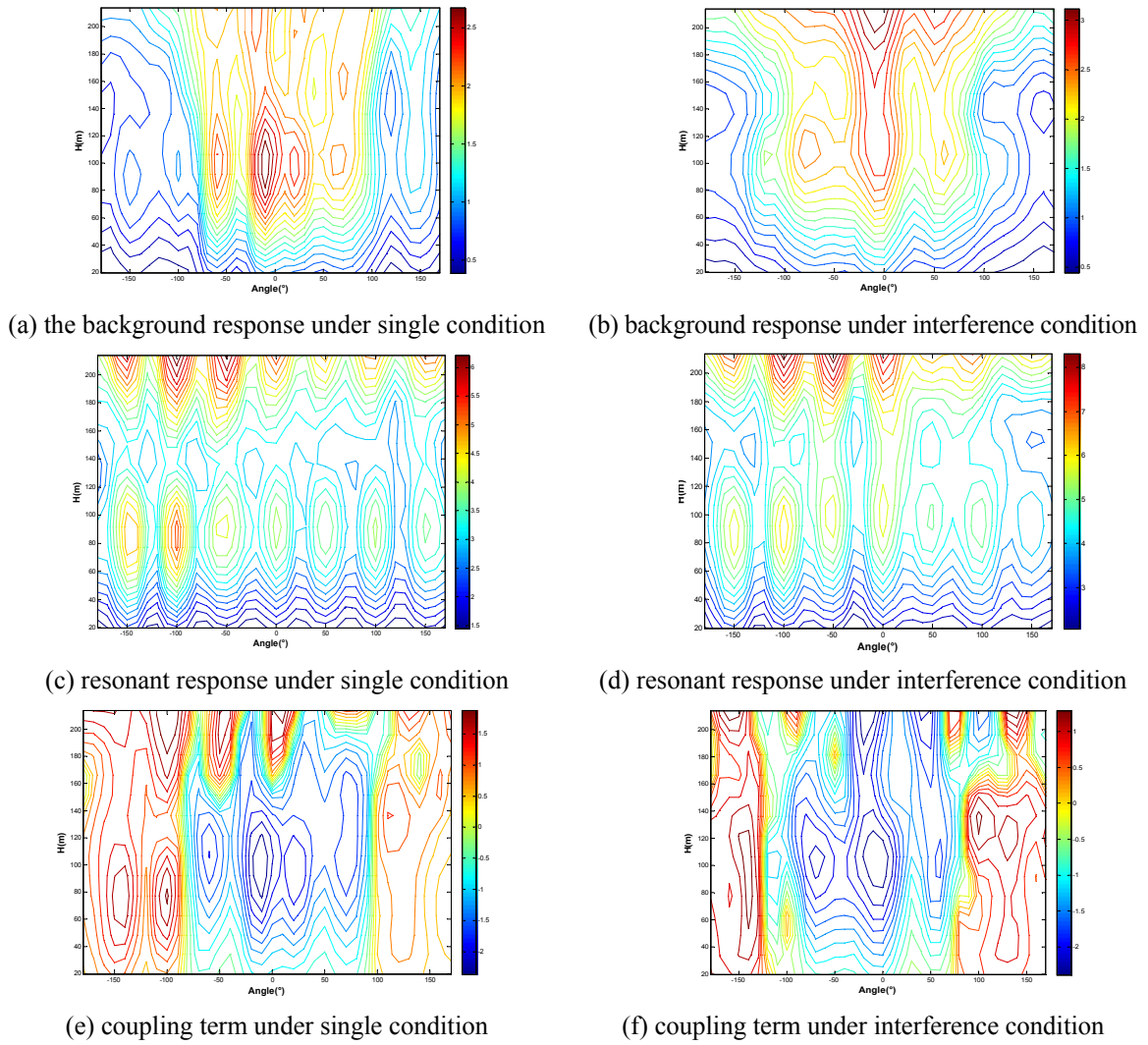


Fig. 9 The contour map of component terms under single condition and interference

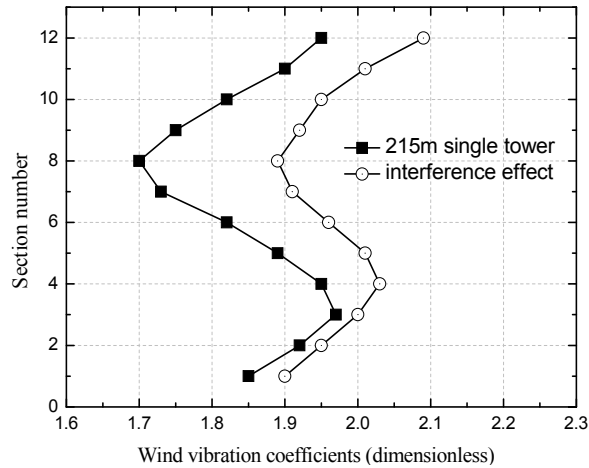


Fig. 10 The influence of the interference effect on the average wind vibration coefficient

section. The interference effect on the fluctuating response values and the distribution characteristic is mainly aimed to state the influence of wind-induced interference mechanism of the cooling towers. As the influence of interference makes the windward area, negative pressure extremum area and leeward area of the cooling tower unclear, the toroidal area cannot be divided like single cooling tower. So the characteristics distribution of the fluctuating wind vibration response is mainly analyzed in this paper. Fig. 8 gives the power spectrum density function of tower top displacement with and without interference effects. The resonant response component plays a comparatively important role in the total fluctuating response, the contributions from the modes whose frequencies are higher than 20 Hz and 30 Hz to the responses are negligible. The resonant response and background response both increase obviously when considering the interference effect.

The contour map of the wind-induced background, resonant response and coupling term under single condition and interference in the example 3 is showed in Fig. 9. The average wind vibration coefficient curve of the 12 cross sections in the meridian height direction under single condition and interference of the example 3 is showed in Fig. 10.

By the analysis of the contour map of fluctuating wind vibration response components under single condition and interference, when considering interference effect, background and resonant response values of the cooling tower are significantly increased. The increase degree of resonant response, whose peak values increase from 6.4 mm to 8.2 mm, is more significant with growth of 28%. Compared with that, the growth of the background response component is only 10%. The phenomenon shows that the existence of the distractors can greatly increase the dynamic amplification effect of the cooling tower structure, and the increase degree of quasi static contribution portion is relatively small. The wind vibration coefficient presents the change rule that first increases then decreases with the increase of height under single condition and interference. The influence of the interference effect on the wind vibration coefficient at the bottom of cooling tower is small, with the increase of altitude, the interference effect makes the wind vibration coefficient values significantly greater than that under single condition. So the placement form of the surrounding distractors and its optimization should be considered in the actual project.

## 7. Conclusions

- The affecting factors the wind-induced vibration characteristics of cooling towers can be divided into two categories in nature. The first one is the factors of the structure itself, including the size characteristics (such as the height of tower, the thickness of shell, diameter, inlet height, etc.) and the damping ratio. The second one is the interference effect of the surrounding buildings.

- The interference effect has the greatest influence on the fluctuating wind-induced response, which significantly increases the proportion 28% of resonant component, and the proportion 10% of background component. The influence of the interference effect on the wind vibration coefficient at the bottom of cooling tower is weak, but the interference effect greatly increases the wind vibration coefficient in the middle and top regions. The change rule of wind vibration coefficient presents that first increases then decreases until to the throat height, finally increases to the tower top.

- With the decrease of the structural fundamental frequency, the average response and fluctuating response gradually increase, the growth of the fluctuating response is greater than that of average response, the proportion of resonant response becomes more and more significant, and the proportion of the background response gradually decreases. On the other hand, with the decrease of fundamental frequency, the structural size in toroidal and meridian direction increases, which leads to the decrease of spatial correlation of fluctuating wind loads on the surface, making the growth of the wind vibration response relatively lower. So the influence of the two factors on wind vibration response is just the opposite, which leads to the change for the wind vibration coefficient is not obvious when the structural fundamental frequency changes.

- With the increase of the damping ratio, the resonant response of the structure significantly decreases, and its peak value reduces from 9.4 to 4.5 mm. The reason is that the resonant response is dominant in the wind vibration response of the large tower structure, but in the meridian to the height and circular cross section on the response distribution characteristics of basic consistent, that stimulates the resonant response of dominant mode has not changed. However, the response distribution characteristics at the meridian height and the toroidal cross section is basic consistent, which instructs that dominant mode stimulating the resonant response has not changed.

## Acknowledgments

This project is jointly supported by National Natural Science Foundation (50978203 and 51208254) and Jiangsu Province Natural Science Foundation (BK2012390), and Postdoctoral Science Foundation (2013M530255; 1202006B), which are gratefully acknowledged.

## References

- Bartoli, G., Borri, C., Hoeffler, R. and Orlando, M. (1997), "Wind induced pressures and interference effects on a group of cooling towers in a power plant arrangement", *Proceedings of 2nd European and African Conference on Wind Engineering*, Genoa, Italy, Padua.
- Busch, D., Harte, R., Kraetzig, W.B. and Montag, U. (2002), "New natural draught cooling tower of 200 m height", *Eng. Struct.*, **24**(12), 1509-1521.
- DL/T 5339-2006 (2006), "Code for hydraulic design of fossil fuel power plants", Standard National Development and Reform Commission, 58-61.

- Goodarzi, M. (2010), "A proposed stack configuration for dry cooling tower to improve cooling efficiency under crosswind", *J. Wind Eng. Ind. Aerodyn.*, **98**(12), 858-863.
- Harte, R. and Wittek, U. (2009), "Recent developments of cooling tower design", *Proc. of IASS Symposium*, Valencia, Spain, September-October.
- Holmes, J. (2002), "Effective static load distributions in wind engineering", *J. Wind Eng. Ind. Aerodyn.*, **90**(2), 91-109.
- Kasperski, M. and Niemann, H.J. (1992), "The LRC (load-response correlation) method: a general method of estimating unfavorable wind load distributions for linear and nonlinear structural behavior", *J. Wind Eng. Ind. Aerodyn.*, **43**, 1753-1763.
- Ke, S.T., Ge, Y.J., Zhao, L. and Tamura, Y. (2013), "Wind-induced responses characteristics on super-large cooling towers", *J. Centr. South Univ. Tech.*, **20**(11), 3216-3227.
- Ke, S.T., Ge, Y.J., Zhao, L. and Tamura, Y. (2012), "A new methodology for analysis of equivalent static wind loads on super-large cooling towers", *J. Wind Eng. Ind. Aerodyn.*, **111**(3), 30-39.
- Li, G. and Cao, W.B. (2013), "Wind-induced response of large hyperbolic cooling tower considering soil-structure interaction", *Struct. Eng. Mech.*, **46**(5), 164-176.
- Mohammad-Ali, G. and Saeed-Reza, S.Y. (2008), "Modeling wind ribs effects for numerical simulation external pressure load on a cooling tower of Kazerun power plant-Iran", *Wind Struct.*, **11**(6), 479-496.
- Noh, S.Y., Kratzig, W.B. and Meskouris, K. (2003), "Numerical simulation of serviceability, damage evolution and failure of reinforced concrete shells", *Comput. Struct.*, **81**(11), 843-857.
- Niemann, H.J. and Kopper, H.D. (1998), "Influence of adjacent buildings on wind effects on cooling towers", *Eng. Struct.*, **20**(10), 874-880.
- Orlando, M. (2001), "Wind-induced interference effects on two adjacent cooling towers", *Eng. Struct.*, **23**, 979-992.
- Qiao, Q., Guo, Z. and Wang, R. (2011), "Wind tunnel experimental study on effect of nuclear power plant cooling tower on radioactive plume dispersion", *Bioinformatics and Biomedical Engineering, (iCBBE) 2011 5th International Conference on. IEEE*, 1-6.
- Ramakrishnan, R. and Arumugam, R. (2012), "Optimization of operating parameters and performance evaluation of forced draft cooling tower using response surface methodology (RSM) and artificial neural network (ANN)", *J. Mech. Sci. Tech.*, **26**(5), 1643-1650.
- Sun, T.F. and Gu, Z.F. (1992), "Full-scale measurement and wind-tunnel testing of wind loading on two neighboring cooling towers", *J. Wind Eng. Ind. Aerodyn.*, **43**(1-3), 2213-2224.
- VGB-Guideline (2005), "Structural design of cooling tower- technical guideline for the structural design, computation and execution of cooling towers", Standard Essen, BTR Bautechnik bei Kühltürmen.
- Zahlten, W. and Borri, C. (1998), "Time-domain simulation of the non-linear response of cooling tower shells subjected to stochastic wind loading", *Eng. Struct.*, **20**(10), 881-889.
- Zhang, J.F., Chen, H., Ge, Y.J., Zhao, L. and Ke, S.T. (2014), "Effects of stiffening rings on the dynamic properties of hyperboloidal cooling towers", *Struct. Eng. Mech.*, **49**(5), 619-629.
- Zhao, L. and Ge, Y.J. (2010), "Wind loading characteristics of super-large cooling towers", *Wind Struct.*, **13**(4), 257-274.